NASA/TM-20260000705

# Manufacturing Process Development of a Carbon Fiber Reinforced Polymer Composite Shaft for Electric Motors

*Joseph Pinakidis, Sandi Miller, Thomas Tallerico, and Jonathan Salem*
*Glenn Research Center, Cleveland, Ohio*

*Brandon Strohminger, Nathan Jessie, and Zachary Cahill*
*A&P Technology, Cincinnati, Ohio*

*Adam Elsmore and Scott Nielson*
*Origen Manufacturing, Pleasant View, Utah*

February 2026

# NASA STI Program Report Series

Since its founding, NASA has been dedicated to the advancement of aeronautics and space science. The NASA scientific and technical information (STI) program plays a key part in helping NASA maintain this important role.

The NASA STI program operates under the auspices of the Agency Chief Information Officer. It collects, organizes, provides for archiving, and disseminates NASA's STI. The NASA STI program provides access to the NTRS Registered and its public interface, the NASA Technical Reports Server, thus providing one of the largest collections of aeronautical and space science STI in the world. Results are published in both non-NASA channels and by NASA in the NASA STI Report Series, which includes the following report types:

- TECHNICAL PUBLICATION. Reports of completed research or a major significant phase of research that present the results of NASA programs and include extensive data or theoretical analysis. Includes compilations of significant scientific and technical data and information deemed to be of continuing reference value. NASA counterpart of peer-reviewed formal professional papers but has less stringent limitations on manuscript length and extent of graphic presentations.

- TECHNICAL MEMORANDUM. Scientific and technical findings that are preliminary or of specialized interest, e.g., quick release reports, working papers, and bibliographies that contain minimal annotation. Does not contain extensive analysis.

- CONTRACTOR REPORT. Scientific and technical findings by NASA-sponsored contractors and grantees.

- CONFERENCE PUBLICATION. Collected papers from scientific and technical conferences, symposia, seminars, or other meetings sponsored or cosponsored by NASA.

- SPECIAL PUBLICATION. Scientific, technical, or historical information from NASA programs, projects, and missions, often concerned with subjects having substantial public interest.

- TECHNICAL TRANSLATION. English-language translations of foreign scientific and technical material pertinent to NASA's mission.

Specialized services also include organizing and publishing research results, distributing specialized research announcements and feeds, providing information desk and personal search support, and enabling data exchange services.

For more information about the NASA STI program, see the following:

- Access the NASA STI program home page at http://www.sti.nasa.gov

NASA/TM-20260000705

# Manufacturing Process Development of a Carbon Fiber Reinforced Polymer Composite Shaft for Electric Motors

*Joseph Pinakidis, Sandi Miller, Thomas Tallerico, and Jonathan Salem*
*Glenn Research Center, Cleveland, Ohio*

*Brandon Strohminger, Nathan Jessie, and Zachary Cahill*
*A&P Technology, Cincinnati, Ohio*

*Adam Elsmore and Scott Nielson*
*Origen Manufacturing, Pleasant View, Utah*

National Aeronautics and
Space Administration

Glenn Research Center
Cleveland, Ohio 44135

February 2026

*Level of Review*: This material has been technically reviewed by technical management.

This report is available in electronic form at https://www.sti.nasa.gov/ and https://ntrs.nasa.gov/

NASA STI Program/Mail Stop 050
NASA Langley Research Center
Hampton, VA 23681-2199

# Manufacturing Process Development of a Carbon Fiber Reinforced Polymer Composite Shaft for Electric Motors

Joseph Pinakidis, Sandi Miller, Thomas Tallerico, and Jonathan Salem
National Aeronautics and Space Administration
Glenn Research Center
Cleveland, Ohio 44135

Brandon Strohminger, Nathan Jessie, and Zachary Cahill
A&P Technology
Cincinnati, Ohio 45245

Adam Elsmore and Scott Nielson
Origen Manufacturing
Pleasant View, Utah 84404

## Abstract

Electric aircraft applications require electric motors with increased specific power and efficiency. Composite structural components in motors are a potential solution for reducing motor mass, reducing magnetic losses, and limiting undesired conduction paths for fault, electromagnetic interference, or common-mode currents. In this report, manufacturing trials for a high-speed carbon fiber reinforced polymer composite motor shaft are presented. Four prototype shafts were produced using a hybrid biaxial/triaxial fabric that was circumferentially wrapped onto an additively manufactured high-temperature washout mandrel. An additional traditional overbraid approach was also evaluated and shows promise for high-rate, high-performance parts using automated manufacturing. This paper discusses the shaft design, manufacturing methods explored, material selection, the manufacturing trials, and the lessons learned. The results of this manufacturing investigation show feasibility for manufacturing composite shafts for electric motors.

## 1.0 Introduction

Electric and hybrid electric aircraft require high-performance and reliable electric motors and drivetrains. Lightweight motor structural components with high strength and stiffness, low electrical conductivity, and high thermal conductivity can reduce motor weight and operating temperature while mitigating stray magnetic losses and eliminating possible failure modes. Composites are a potential lightweight material solution for electric motor structures because they offer high ratios of strength and stiffness to weight and reduced bulk electrical conductivity relative to metallic components (Ref. 1). Additionally, they enable more flexible design of motor structural components and geometries that cannot be achieved in a cost-effective manner with traditional manufacturing methods (Ref. 2). Previous manufacturing investigation has shown braiding to be a cost-effective and efficient manufacturing method for composite shafts (Refs. 3 and 4). This will be expanded upon in this work as both a hybrid fabric overwrap and traditional overbraid manufacturing approach are explored.

Carbon fiber composites have been used extensively in electric motors for containment of rotating magnetic components under centripetal loads because they offer thinner structures and, in most cases, lower magnetic loss relative to metallic retaining hoops (Refs. 5 and 6). Carbon fiber shafting has been explored for various automotive and aerospace applications (Refs. 7, 8, and 9). In Gutknecht et al. (Ref. 7), carbon fiber shaft design for electric motors was explored with the goals of reducing stray magnetic loss in the motor shaft, reducing weight, and reducing conductivity for rotor currents that can lead to premature bearing failure. Additional carbon fiber shaft design work investigated design parameters and found that cross-ply laminates with functional grading construction broadens the boundary stability and optimizes for the highest rotational speed (Ref. 10). As for the mandrel, additive manufacturing was leveraged because of its advantages in geometric tailorability, shorter lead time, low cost, and fewer parts (Ref. 11). A high-temperature, 3D-printed washout mandrel was ideal for this iterative and developmental work.

In this report, manufacturing trials of a carbon fiber shaft based on the work of Gutknecht et al. (Ref. 7) are described. An updated carbon fiber shaft design based on manufacturing considerations and an updated optimization model are presented. Manufacturing considerations, methods, and material selections are discussed. Four prototype shafts were produced using a hybrid fabric overwrap method. The prototypes are intended as proof-of-concept shafts demonstrating shaft manufacturing feasibility and enabling validation of modal frequencies.

## 2.0 Design

Relative to the shaft and motor design presented in Reference 7, a new motor and shaft design was generated for the manufacturing trials. The overdesign of the shaft in Reference 7 for modal frequency, as well as concerns of manufacturing feasibility for the original shaft geometry, led to the redesign. From manufacturing discussions, updates to the carbon fiber directions and constraints on the relative diameter of the bearings and magnets were integrated into the motor design tool. A finite element analysis (FEA) model of the shaft was added to replace the analytical design of the shaft in the motor design tool; see Figure 1. The FEA model enabled better representation of the shaft geometry and the changes in effective carbon fiber composite material properties as the shaft changes diameter and the carbon fiber directions changed within the composite. The FEA model predicted an eigenfrequency of 1,149.7 Hz for the part.

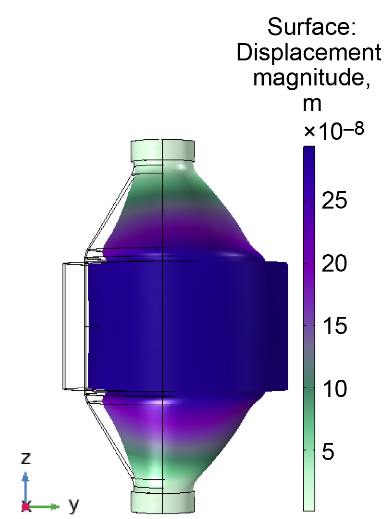


Figure 1.—Shaft FEA modal analysis integrated into motor design tool for carbon fiber shafts. Eigenfrequency = 1,149.7 Hz.

Apart from the added FEA model and the updated geometry constraints, all other parts of the design tool described in Reference 7 were maintained and the motor was reoptimized. Figure 2 shows the optimization results for a 100-kW motor. Relative to the results in Reference 7 for carbon fiber shafted flux-focusing motors, similar performance is achieved with the updated models. The FEA model significantly slowed down the optimization, however, and correspondingly, the pareto front is less converged for the optimization. Additionally, the integration of the FEA model and constraint on motor geometry resulted in an appreciably faster motor speed being optimum. The lightest designs in Figure 2 spin at rpms between 15,000 and 20,000, whereas the results in Reference 7 had the lightest designs at a rotational speed between 3,000 and 15,000 rpm.

From the design optimization results, a design was selected to prototype the shafts. Figure 3 shows the prototype motor geometry. The selected machine design has a nominal rotational speed of 15,860 rpm and is predicted to achieve a specific power of roughly 10 kW/kg at an efficiency of 96.6%. Figure 4 shows the shaft design drawings. The following sections discuss prototyping trials for the shaft.

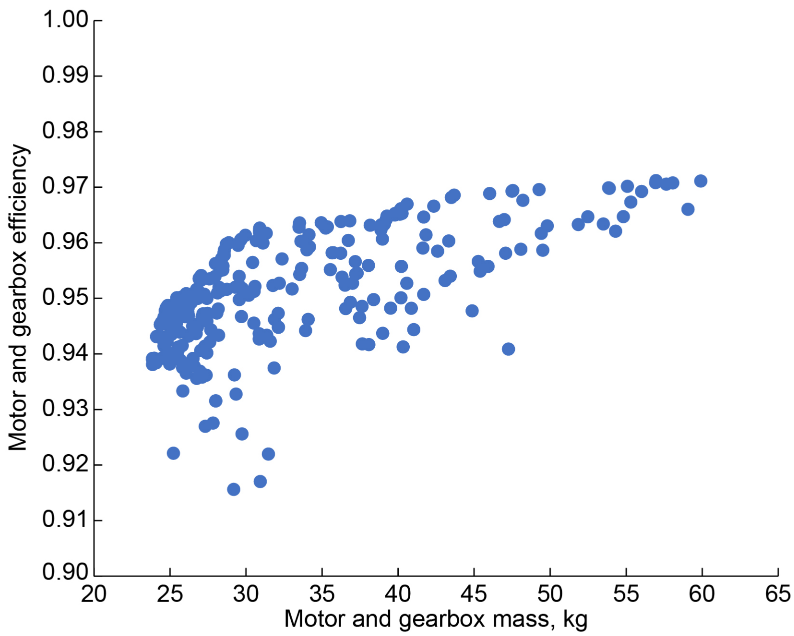


Figure 2.—Optimization results for updated design.

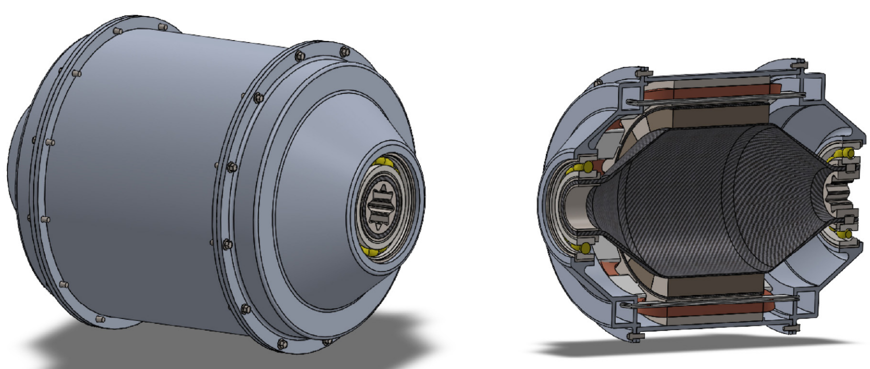

(a) (b)

Figure 3.—Updated motor design geometry. (a) Entire part within motor casing. (b) Cross-sectional view of shaft assembly integrated into electric motor application.

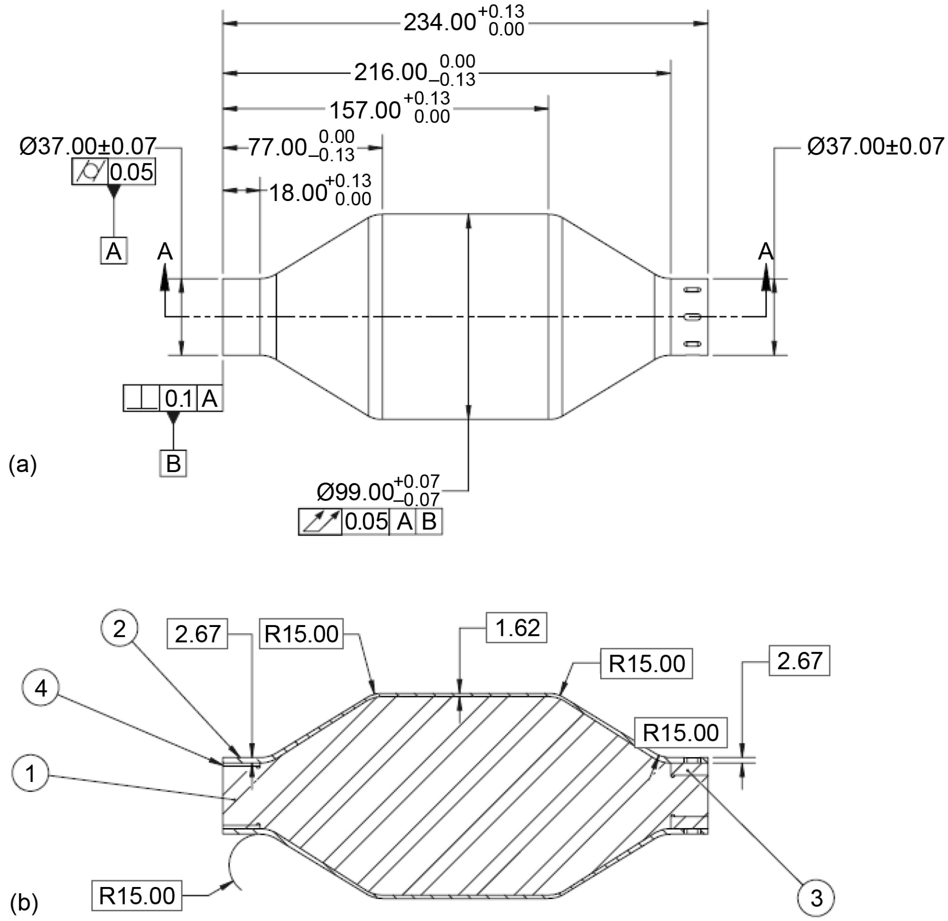


Figure 4.—Carbon fiber shaft engineering drawings; dimensions in mm. (a) Exterior dimensions of entire part. (b) Cross-sectional view of part: 1, washout mandrel; 2, shaft; 3, premachined output side-bearing ID sleeve; 4, inner shaft sleeve, input side.

## 3.0 Manufacturing Methods

Two manufacturing methods were selected to prototype the shaft: (1) a hybrid fabric overwrap and (2) a traditional overbraid. T700S carbon fiber with 12k filaments per tow from Toray was used for the reinforcement material in both manufacturing approaches. A bismaleimide (BMI) resin, CYCOM® 5250-4 resin, was used because it is compatible with the typical operating temperatures of high-performance electric motors. CYCOM® 5250-4-BMI has an operating range temperature of –59 to 204 °C (–75 to 400 °F). All manufacturing of the carbon fiber shafts, excluding the washout mandrels, was performed by A&P Technology.

To enable the hollow shaft geometry with both manufacturing methods, a 3D-printed washout mandrel was selected from Origen Manufacturing. The washable mandrel simplifies tooling development for the hollow shaft and enables manufacturing of the shaft as one piece. 3D printing reduced the manufacturing costs for this prototype effort and enabled higher design flexibility with each iteration. A ceramic (synthetic CB-X 1450 from Cera Tec) material was selected for the mandrel material to enable compatibility with the infusion temperature of the BMI resin. Once printed, the mandrel was rated to a temperature of 204 °C (425 °F). Its water-soluble binder is both nontoxic and environmentally friendly. Figure 5 shows the mandrels after printing.

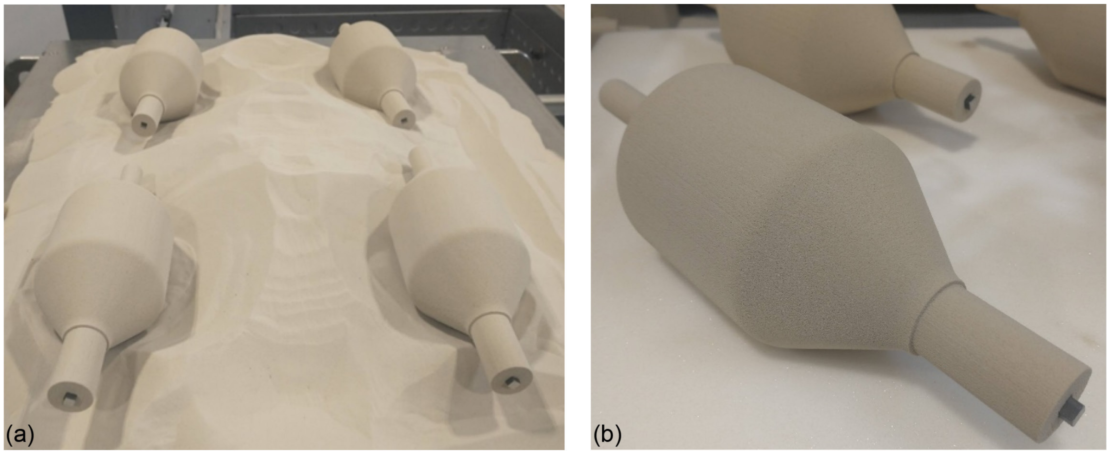


Figure 5.—Additively manufactured high-temperature washout mandrels from Origen Manufacturing; manufactured using porous media (air and ceramic). (a) Still in powder bed after being additively manufactured. (b) Close-up side view.

The design of the resin infusion geometry for the shaft is shown in Figure 6(a). The mandrels were designed to extend longer on each end of the actual shaft to enable integration of alignment and infusion geometry. The extended, central metal key stock was necessary to keep the mandrel centered during the manufacturing process and aligned, as both methods required precise start and stop locations for their respective braiding techniques. The added length also enables the shaft to be cut to length after resin infusion. The alignment jig incorporated holes at the ends of the shaft to allow for resin and entrapped air to be evacuated during the resin infusion and curing process by pulling vacuum on these holes. A 0.25-in. key stock bar is inserted through the center to hold the mandrel during the wrapping processes.

As shown in Figure 6(b), inner and outer bearing sleeves are included in the resin infusion assembly of the shaft. These bearing sleeves are included to provide the correct stiffness for the bearings, enable postprocess machining of the bearing seats to their desired tolerance, and enable mechanical connections to the motor shaft. Before applying carbon fiber to the mandrel, the inner bearing sleeve was abraded with 70-grit black aluminum oxide to provide better adhesion for the resin system used. The surface was then wiped clean with acetone, and Cytec BR® 127 corrosion-inhibiting primer was applied shortly afterward. BR® 127 not only prevents rust, which would be considered a contaminant in this application, but further prepares the surface for the resin to adhere appropriately. The same process was used to prepare the bearing outer sleeve prior to installing it onto the carbon fiber after wrapping.

The high-temperature ceramic mandrel with silicone coating had a 6.35-mm-thick (0.25-in.) steel square axle running through the centerline of the part. The ends of the axel were inserted into square slotted jigs to hold the mandrel in place. Once the position of the mandrel was set, the slotted jigs were secured to prevent any translational movement during the taping and overwrapping process; see Figure 7.

Before resin infusion, the 3D-printed ceramic mandrel was coated in silicone to prevent infiltration by the BMI infusion resin. A release layer of PTFE tape was applied to the outside of the silicone before the braided carbon fiber was applied. Figure 7 shows the mandrel after being prepared for fiber wrapping.

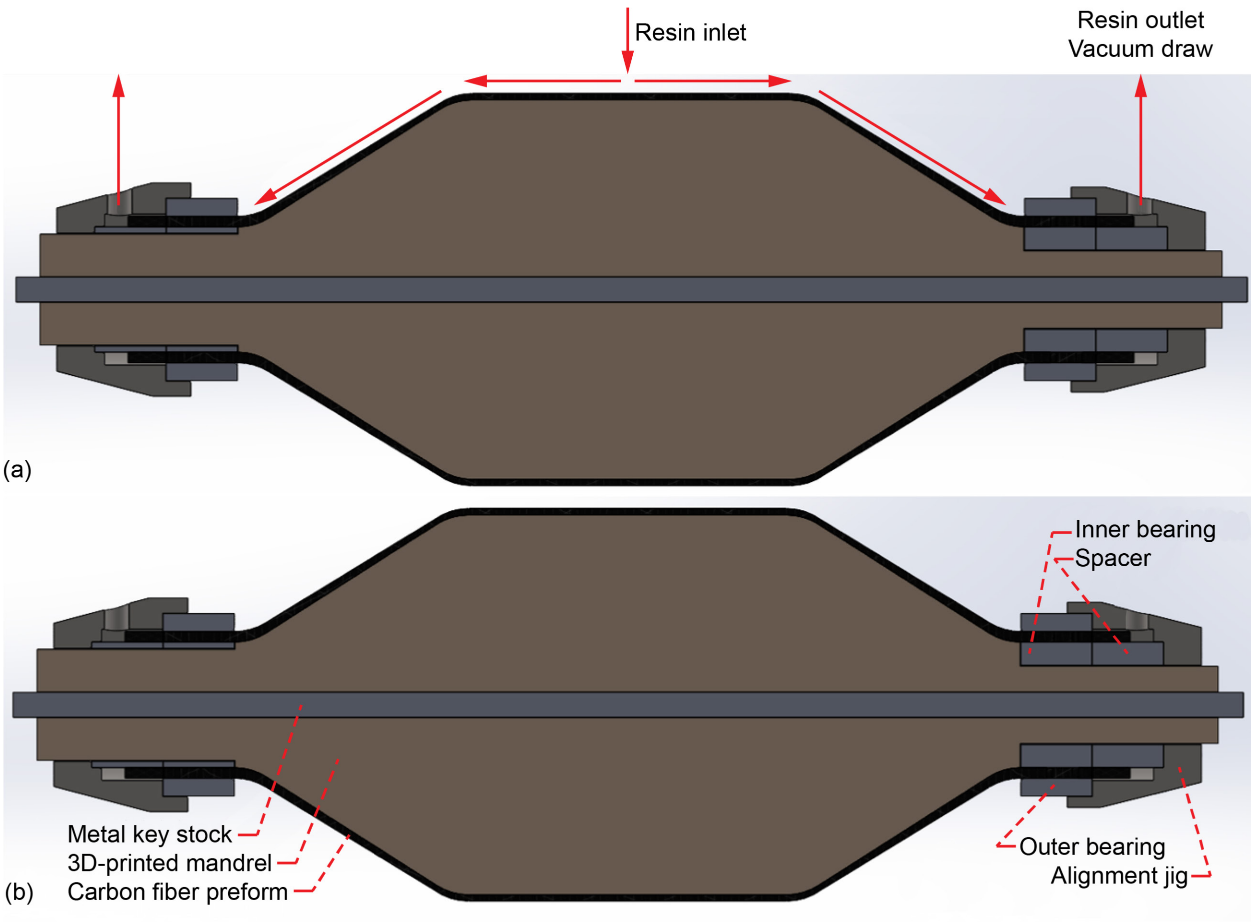


Figure 6.—Carbon fiber preform on 3D-printed mandrel. (a) Resin infusion plan. (b) Alignment jig with bearings.

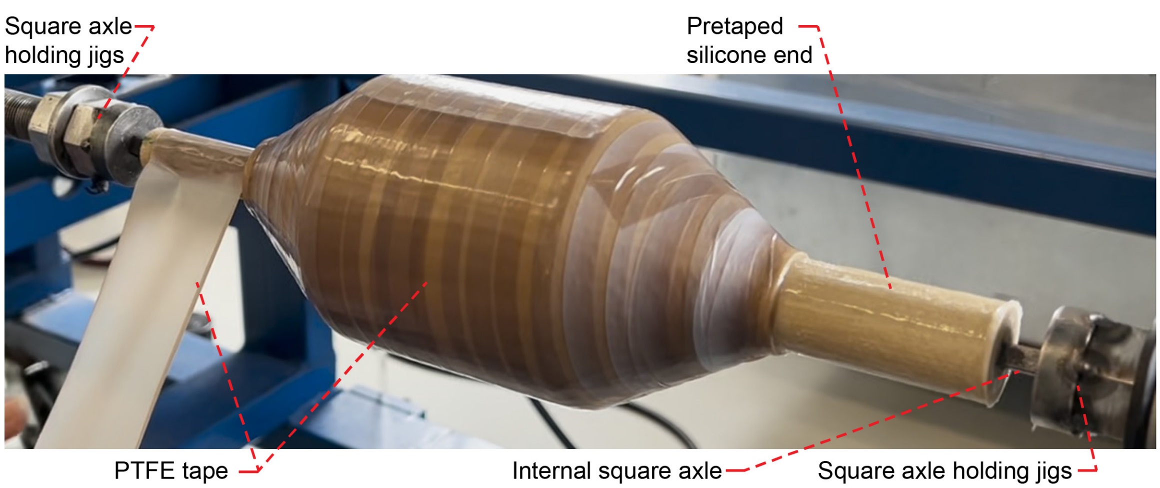


Figure 7.—PTFE tape application onto mandrel.

## 3.1 Hybrid Fabric Overwrap Approach

In the hybrid fabric overwrap approach, carbon fiber fabric was wrapped circumferentially around the mandrel. Figure 8 shows the hybrid fabric and its fiber layout over the length of the mandrel. The center region with a larger diameter is triaxially braided with ±45° bias directions. It is important to note that in the fabric overwrap method, the 0° direction is defined as the direction wrapped circumferentially around the hoop of the shaft in the center section of the mandrel. Biaxial braid is used for both shaft ends and under the bearing seat to better conform to the sloping region and changing diameter size. The biaxial bias angles self-align and range from ±45° at the outer diameter of the shaft to ±76.7° at the bearing location. A visualization of the fiber overwrap process is documented in Figure 9. The image details the manufacturing process for the overwrap approach, including a compaction roller, laser-projected start/stop, back-tensioned payoff reel, and the triaxial/biaxial regions of the carbon fiber preform.

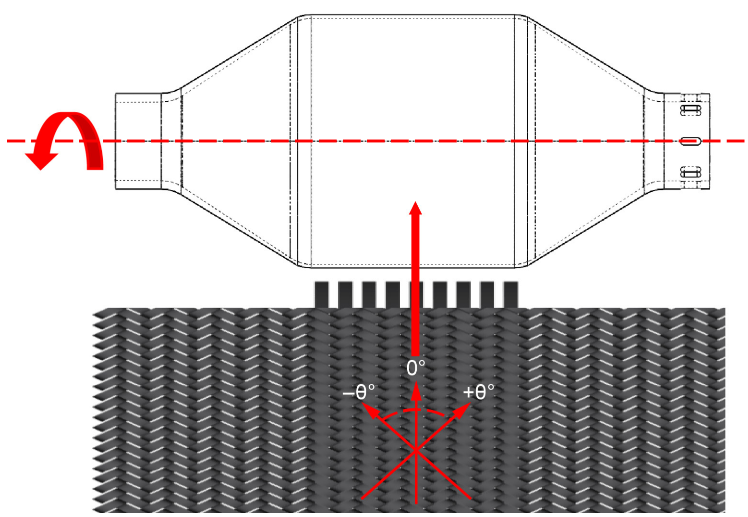


Figure 8.—Hybrid triaxial/biaxial fabric overwrap approach.

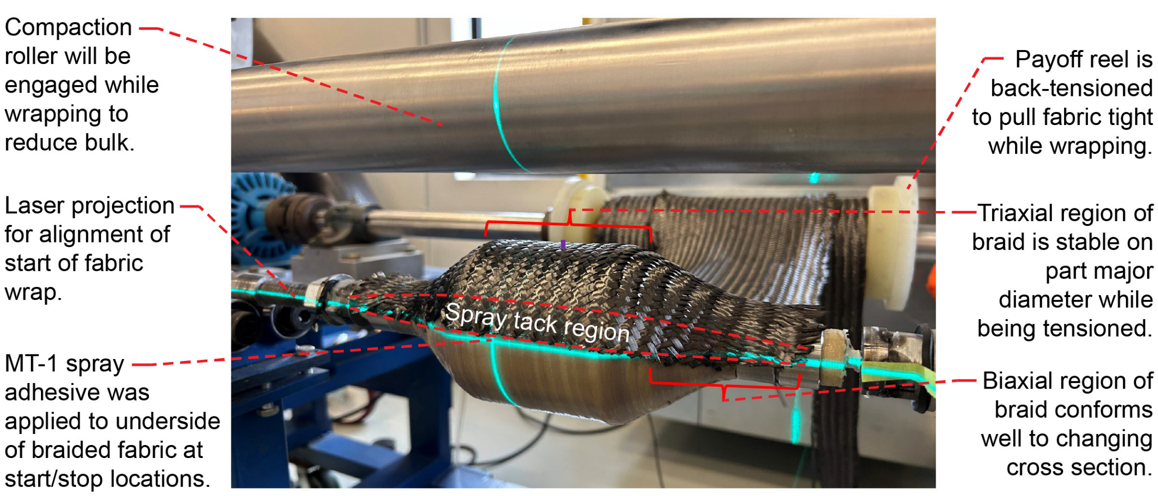


Figure 9.—Hybrid biaxial/triaxial carbon fiber overwrap method with fabric applied circumferentially onto mandrel.

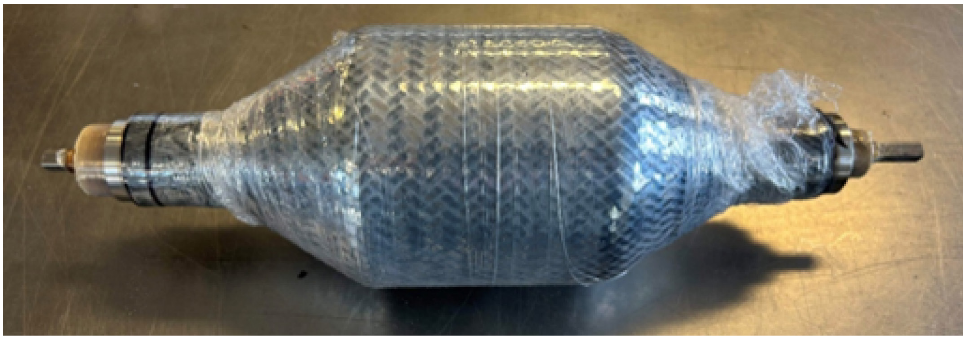

Figure 10.—Overwrapped mandrel with debulking plastic wrap layer prior to resin infusion.

Extreme care was taken during the overwrapping process to ensure that the seams lined up with each other for good part fidelity. After the fabric was wrapped three times over the ceramic sand mandrel, an epoxy acetone spray was applied to the slanted ramps of the part to add rigidity to the fabric during resin infusion. After the epoxy acetone mixture was applied, plastic shrink wrap was wrapped tightly around the preform (Figure 10) to debulk it overnight. The shrink wrap was removed the following morning to give enough time for the acetone to flash off. Once the plastic wrap was removed, the outer metallic bearings were fit over the ends of the braided part.

Advantages of the fabric overwrap method include a lower upfront cost as compared to overbraiding, but additional labor is required to wrap the fabric around the sand mandrel. Depending on the applications, the cost of labor can greatly increase the overall cost to produce an overwrapped part. Other drawbacks of the hybrid overwrap method include difficulty in keeping the fabric pulled tight to prevent wrinkles when wrapping, and the emergence of a seam at the start and stop regions. In the current stage of development for this fabric overwrap technique, it is difficult to get the start and stop seams to perfectly line up so that the finished product is completely flush and symmetrical. This is an area of improvement that is expected to be refined with additional manufacturing development.

### 3.2 Traditional Overbraid Approach

For the traditional overbraid method, the fiber tows were braided onto the mandrel as it was axially fed through a 36-carrier braid machine. In this method, the 0° axial fibers follow the center axis of the part. The bias fibers changed directions from ±45° at the shaft center to ±75° at the bearing locations. The bias angles had to adjust throughout the shaft at nine stations to accommodate a changing diameter size and sloping region; see Figure 11. The traditional overbraid is visualized in Figure 12. Images are prior to resin infusion.

Directly overbraiding the mandrels has many advantages over hand-layup. Overbraiding the layers is an automated process that is machine controlled and highly repeatable, which reduces variability of the layup. Every carbon fiber tow is equally tensioned and pulled tight to the mandrel, which debulks the preform as it is being produced. The overbraid fiber architecture is also continuous around the circumference of the part, so there are no seams or splices in the reinforcement. This will increase performance of the part and produce a highly symmetric preform, whereas the circumferentially wrapped preform will have a seam that needs to be managed and can introduce asymmetry. The overbraid approach allows for high-rate, repeatable, and automated production of the carbon fiber preform.

Due to the number of prototyping iterations completed in this project, as well as scheduling and budget constraints, none of the final prototypes were produced using the overbraid method. Its benefits, however, potentially make it a better approach than the overwrap method for volume production and performance of motor shafts.

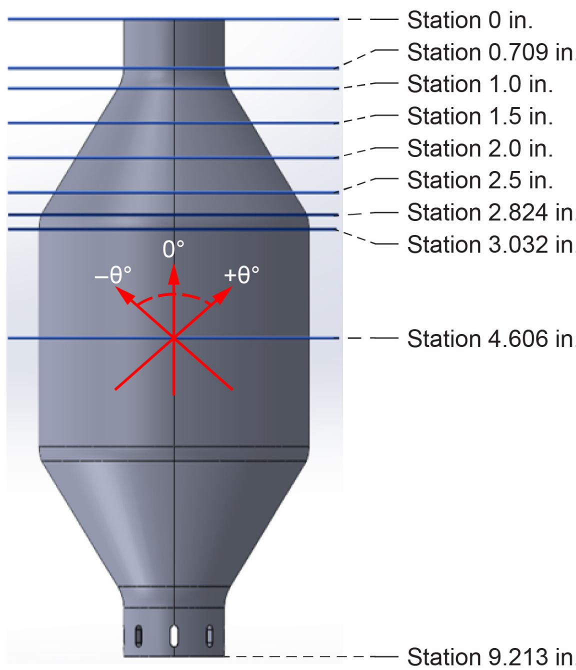


Figure 11.—Mandrel for traditional overbraid approach. There are 9 stations intended to change the angle of the bias tows to accommodate changing diameter size.

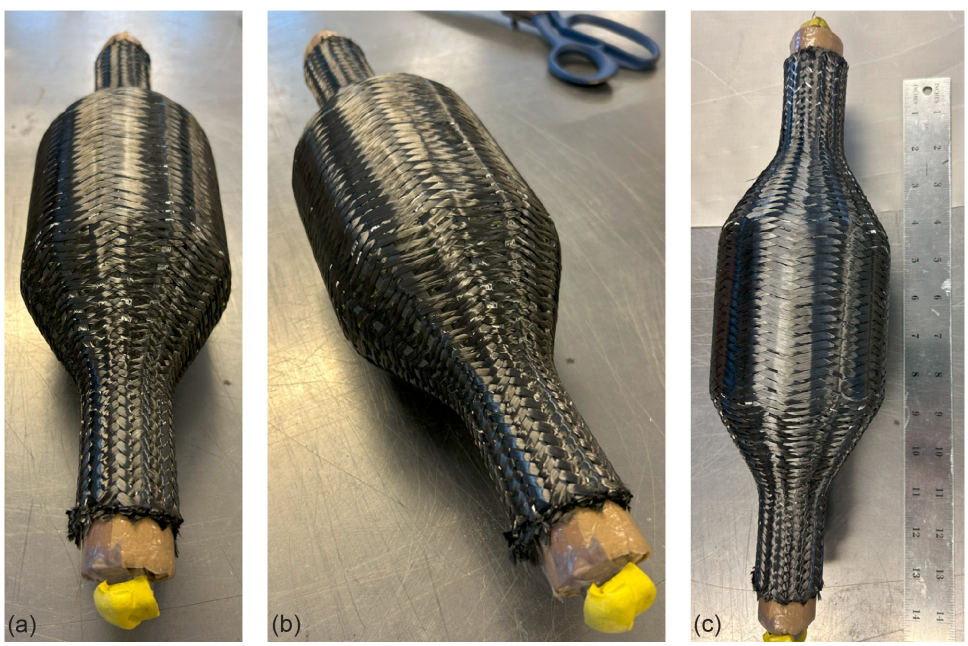


Figure 12.—Traditional fiber overbraid on first-generation mandrel prior to resin infusion.

### 3.3 Resin Infusion Process

After the dry carbon fiber preform was laid up onto the mandrel, the full assembly was bagged for resin infusion. The first step of the bagging process was to apply a peel ply layer. The purpose of peel ply is to allow easier removal of the vacuum bag and the flow media once the curing process has finished. As seen in Figure 13, one layer of peel ply was wrapped around the part. The ramp sections were cut into petal formations to make the peel ply easier to conform to the sloping geometry. Fibertack MT-1 was sprayed on the peel ply before the petal was adhered to the ramp of the braided part.

The next step of the bagging process involved flow media. Flow media allows resin to flow under and over the fine mesh, allowing an appropriate resin flow during infusion. White polytetrafluoroethylene (PTFE) netting can be seen in Figure 14. Due to the unique shape of this part and the need to wet out appropriately, a flow media “halo” was constructed to hold a spiral tube resin inlet. Without the PTFE halo, the spiral tubing would collapse inward toward the part and would leave a mark-off in the center of the part. Blue flashbreaker tape was tightly wound around the flow media to hold the halo in the desired position, and tan PTFE tape was used to hold down the peel ply petals along the ramps of the part.

The final set of the bagging process was to apply the high-temperature vacuum bag. The bagging was cut with ample sizing to envelop the part, as shown in Figure 15. Yellow tacky tape was then used to seal the bag. If vacuum is applied to the 3D-printed ceramic mandrel, there is risk that resin would infiltrate and cure inside the mandrel, preventing it from being extracted. To mitigate this risk, one end of the mandrel was exposed to the atmosphere so the mandrel was not under vacuum pressure. The vacuum was only intended to be drawn from the silicone coating on the mandrel, through the carbon fiber preform, to the outer vacuum bag.

The resin inlet line was attached to the brass T joint in the tubing located in the center of the part before the top of the bag was sealed off. To ensure that an appropriate vacuum was being held, a barometer was used to test the internal pressure of the bag. Before vacuum was applied, the barometer read approximately 970 hPa (14.0 psi). Additional tacky tape was applied at both ends of the shaft to reduce air leaks once vacuum was pulled; see Figure 16. With a full seal, the internal pressure within the bagging was reduced to between 30 and 65 hPa (0.44 and 0.94 psi). For the four parts produced, approximately 900 hPa (13 psi) was applied during the infusion and curing process.

Figure 13.—Shaft assembly wrapped in peel ply layer.

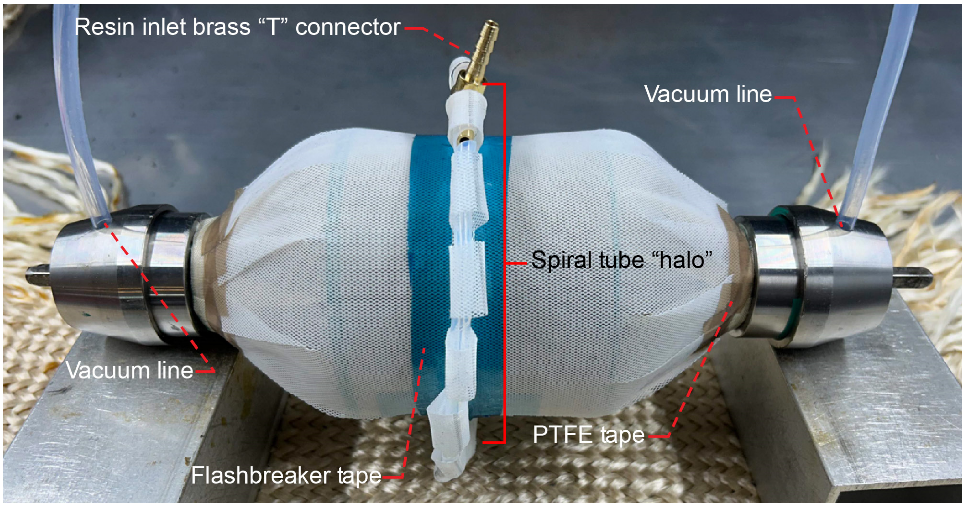

Figure 14.—Carbon fiber shaft with PTFE flow media and resin infusion materials applied.


Figure 15.—Vacuum bagging with part enveloped; not yet sealed.

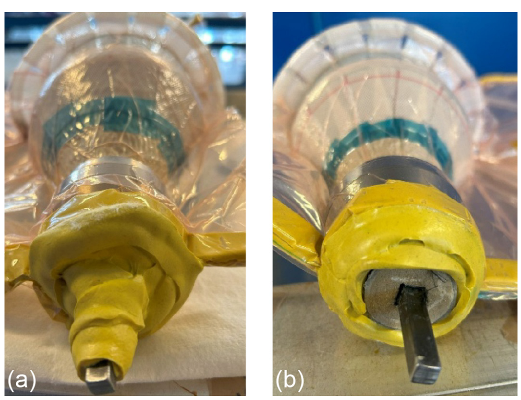

Figure 16.—Tacky tape applied on ends of sand mandrel to maintain vacuum seal. (a) Smaller end. (b) Wider end.

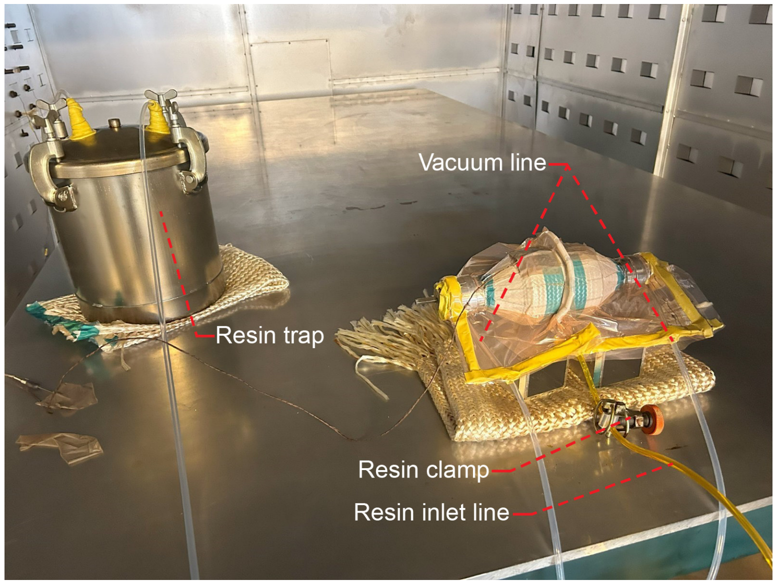

Figure 17.—Part inside oven ready to begin resin infusion process.

The final assembly was placed into an oven and preheated at 121 °C (250 °F) for 2 h while under vacuum. While the part was heating, the BMI resin was preheated to 88 °C (190 °F). After the preform assembly and resin were properly preheated, the resin was infused into the part via vacuum pressure applied at the outlet side of the assembly; see Figure 17.

Once the resin transfer was completed, the clamp was closed and the resin jar was removed. The BMI resin was held for a 6-h cure at 182 °C (360 °F) and gradually reduced to room temperature (23 °C; 73 °F) overnight to cool.

## 3.4 Internal Mandrel Washout and Freestanding Post-Cure

After the resin infusion process was completed, the internal 3D-printed ceramic mandrel was washed out with water; see Figure 18. Once the mandrel was washed out, the internal silicone resin boundary layer and PTFE tape release layer were also removed, leaving behind a hollow carbon fiber composite shaft, as seen in Figure 19. A final, freestanding post-cure was performed to finalize the resin's crosslinking chains. An initial ramp rate of 2.22 °C (4 °F)/min was applied until the part reached 163 °C (325 °F). The ramp was then reduced to 0.28 °C (0.5 °F)/min until 243 °C (470 °F). The part was held at 243 °C (470 °F) for 6 h and gradually reduced to room temperature (23° C) overnight. Once the post-cure process was finished, the final carbon fiber shafts had an operating temperature of –59 to 204 °C.

Figure 18.—Mandrel being washed out in water bucket; entire CF shaft assembly was left to soak in bucket for 1 h until fully washed out.

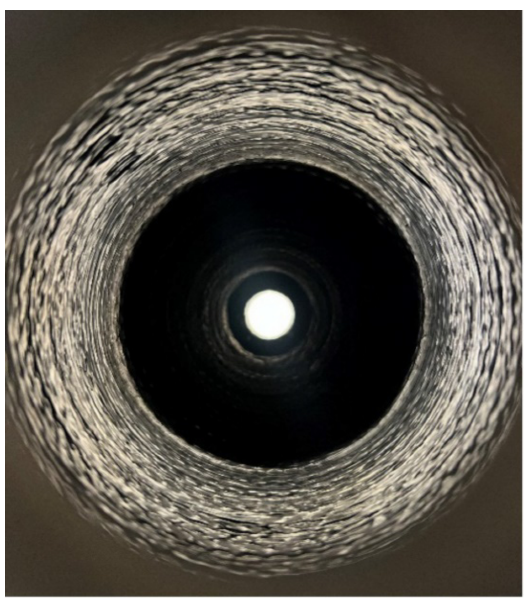

Figure 19.—Hollow interior of carbon fiber shaft after mandrel has been washed out and internal layup materials removed.


Figure 20.—Completed carbon fiber mandrels, all using hybrid fabric overwrap method; bearings installed on ends. (a) One finished part laid horizontally. (b) All four parts next to each other. Shafts had average mass of 140 g without bearings. Combined weight of four bearings was 248 g. Total system mass (shaft plus bearing) was 387 g per finished part.

# 4.0 Results

In total, four carbon fiber shafts were successfully manufactured using the hybrid fabric overwrap method; see Figure 20. Due to the bagging technique and negative pressure applied, some areas of the mandrel were fully wetted out while a few smaller regions remained locally dry. Overall, the shafts held their form after the mandrel had been washed out, which was satisfactory for the goal of manufacturing an initial prototype. After post-cure, each end of the carbon composite shaft was trimmed down to be flush with the bearing sleeves. The total mass of the prototype, shaft and bearings combined, was 387 g. The mass of the four bearings included in each prototype was 248 g. On average, the mass of the carbon fiber shaft was 140 g, which was roughly the same as the design mass of 142 g.

## 4.1 Nondestructive Evaluation

Small regions of porosity were visible at the ends of the CF shaft, and the part did not appear to be uniformly wetted out on its surface. This porosity was most likely due to the BMI resin off-gassing during the cure process and exacerbated by the negative pressure vacuum bagging system utilized. To take a closer look at the internals of the part, nondestructive evaluation with x-ray computed tomography (x-ray CT) was used. The source used was an X-RAY WorX 225-kV microfocus tube operating at 100 kV and 80 µA current. The detector was a Dexela 2923 flat-panel detector with 75-µm pitch and 12 million pixels total. The acquisition and reconstruction was performed with North Star Imaging (NSI) software. Inside the application, the magnification was set to ×1.71, 1800 views, and 43.9-µm voxel size. Cross sections of the CF shaft are visualized in Figure 21.

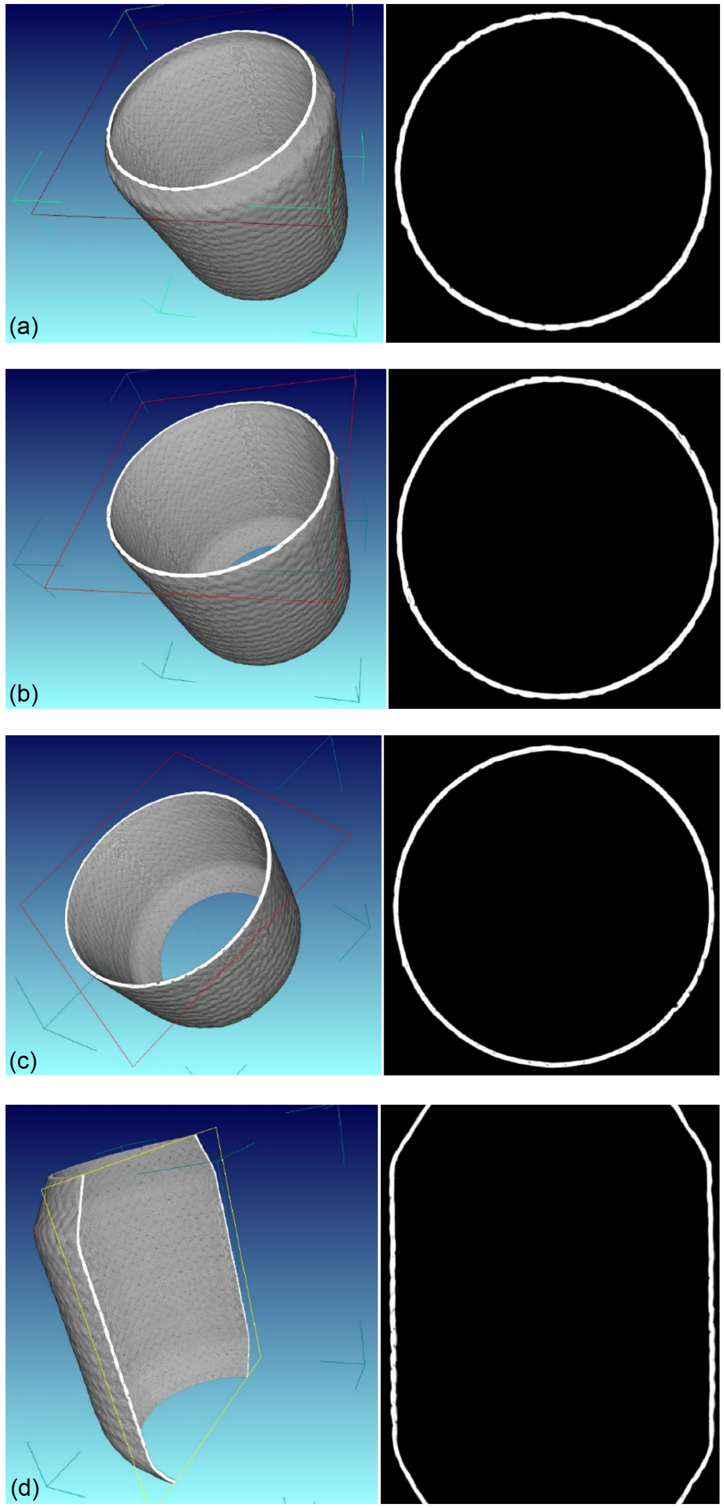

Figure 21.—X-ray CT images of CF shaft. White area represents regions of high consolidation; darker regions represent potential voids or defects. Left side, 3D cross-sectional view of slice on part; right side, corresponding 2D cross-section image. (a) Sloped region. (b) Start of diameter change. (c) Center. (d) Vertical cross-section.

The x-ray CT analysis shows minor porosity scatted through the CF shaft, represented by the darker regions within the white, high-consolidation areas. Overall, NDE analysis qualitatively demonstrates that the shaft is well consolidated in one continuous piece, with some areas to be improved. Cross sections were observed at the sloping region, start of diameter change, center, and vertically, with relatively similar results. This is consistent with the nonuniform surface finish of the shaft that was visually observed.

# 5.0 Conclusions

In this work, four carbon fiber shafts made of T700S carbon fiber and bismaleimide (BMI) resin were successfully fabricated using a hybrid biaxial/triaxial fabric overwrap approach. The produced shafts are intended to show manufacturing feasibility and the viability of carbon fiber shafts for motor applications.

The manufacturing of the shaft was largely enabled by the use of a 3D-printed ceramic washout mandrel. The 3D-printed ceramic mandrel enabled the hollow shaft geometry to be produced with minimal tooling and in one piece. Issues were discovered with the porosity of the 3D-printed mandrel, as resin could penetrate the mandrel during infusion and prevent it from being washed out. This issue was resolved by sealing the mandrel with silicone prior to fiber wrapping. The 3D-printed washout mandrel offers an exciting tool for future prototypes and manufacturing projects.

Two approaches for applying the carbon fiber to the mandrel were explored. Both approaches for creating the braided dry-fiber preform have advantages and disadvantages. The circumferentially hand-applied fabric was found to be easier to iterate quickly. Once the roll of fabric was braided, it was readily available to be applied to different iterations of the 3D-printed mandrels. A major drawback of the circumferentially wrapped fabric is the seam in the reinforcement, which is created at the beginning and end of the spiral-wrapped fabric. Careful alignment of the starting and ending fabric seam had to be managed to ensure there was no gap or overlap that would create a light or heavy spot in the part. The hybrid, biaxial, and triaxial zones of the fabric worked well together to wrap tightly onto the major diameter of the shaft (triaxial zone) and create the end domes of changing part diameter (biaxial zones). Overall, this approach showed promise for quick development cycles but required more manual labor while wrapping the reinforcement, which introduced more variability.

The traditional overbraided preform approach is likely the better approach for shaft manufacturing, as it enables high-rate, automated manufacturing to create the dry fiber preforms. The overbraid approach offers more repeatable and consistent manufacturing as well as the ability to tailor fiber direction across the part. Additionally, due to the continuous nature of the fibers in the overbraid approach, the seams that developed in the wrap approach are avoided. There are, however, more geometric limitations to using the overbraid approach, and the fabric wrap approach may offer greater geometric flexibility.

The BMI resin infusion process used in this work was sufficient for the proof-of-concept prototypes but could be improved substantially for shaft manufacturing. The current scope of work did not allow for a metallic outer mold line clam-shell tool that would have allowed for a positive pressure, resin transfer molding style infusion. The outer clamshell would reduce final part porosity and enable better alignment of the bearing and magnet locations on the outer diameter of the part relative to the bagging process used in this work.

# References


1. Alshammari, B. A., Alsuhybani, M. S., Almushaikeh, A. M., Alotaibi, B. M., Alenad, A. M., Alqahtani, N. B., & Alharbi, A. G. (2021). Comprehensive review of the properties and modifications of carbon fiber-reinforced thermoplastic composites. *Polymers*, *13*(15), 2474.

2. Solomon, D. G., Greco, A., Masselli, C., Gundabattini, E., Rassiah, R. S., & Kuppan, R. (2020, February). A Review on Methods to Reduce Weight and to Increase Efficiency of Electric Motors Using Lightweight Materials, Novel Manufacturing Processes, Magnetic Materials and Cooling Methods. In *Annales de Chimie Science des Matériaux* (Vol. 44, No. 1).
3. Sun, X., Kawashita, L. F., Wollmann, T., Spitzer, S., Langkamp, A., & Gude, M. (2018). Experimental and numerical studies on the braiding of carbon fibres over structured end-fittings for the design and manufacture of high performance hybrid shafts. *Production Engineering*, 12, 215-228.
4. Gude, M., Lenz, F., Gruhl, A., Witschel, B., Ulbricht, A. & Hufenbach, W. (2015). Design and automated manufacturing of profiled composite driveshafts. *Science and Engineering of Composite Materials*, *22*(2), 187-197. https://doi.org/10.1515/secm-2014-0048
5. Gieras, J. F. (2009). *Permanent magnet motor technology: design and applications*. CRC Press.
6. Gallicchio, G., Di Nardo, M., Palmieri, M., Ilkhani, M. R., Degano, M., Gerada, C., & Cupertino, F. (2022). Surface permanent magnet synchronous machines: High speed design and limits. *IEEE Transactions on Energy Conversion*, *38*(2), 1311-1324.
7. Gutknecht, J., Tallerico, T., & Anderson, A., "Design of an In-Slot Cooled Air-Core Flux-Focusing Permanent Magnet Synchronous Machine for Electric Aircraft Applications." NASA/TM – 20240003659, 2024. https://ntrs.nasa.gov
8. Koch, S. F., Peter, M., & Fleischer, J. (2017). Lightweight design and manufacturing of composites for high-performance electric motors. *Procedia CIRP*, *66*, 283-288.
9. Bisht, Y. S., Srikanth, G., Hussain, L., Sanduru, B., Chabra, R., Abdurazakova, N., & Isakulova, B. (2024). Design and modal analysis of composite drive shaft for automotive application. In *E3S Web of Conferences* (Vol. 563, p. 02003). EDP Sciences.
10. Nasr, M. F., Maalawi, K. Y., & Badr, M. A. (2017, July). Optimization of composite drive shafts against whirling instability. In *2017 8th International Conference on Mechanical and Aerospace Engineering (ICMAE)* (pp. 816-821). IEEE.
11. Mehrpouya, M., Vosooghnia, A., Dehghanghadikolaei, A., & Fotovvati, B. (2021). The benefits of additive manufacturing for sustainable design and production. In *Sustainable Manufacturing* (pp. 29-59). Elsevier.